

# A space-time random field model for electricity forward prices

Fred Espen Benth\*      Florentina Paraschiv\*<sup>†</sup>

March 27, 2017

## Abstract

Stochastic models for forward electricity prices are of great relevance nowadays, given the major structural changes in the market due to the increase of renewable energy in the production mix. In this study, we derive a spatio-temporal dynamical model based on the Heath-Jarrow-Morton (HJM) approach under the Musiela parametrization, which ensures an arbitrage-free model for electricity forward prices. The model is fitted to a unique data set of historical price forward curves. As a particular feature of the model, we disentangle the temporal from spatial (maturity) effects on the dynamics of forward prices, and shed light on the statistical properties of risk premia, of the noise volatility term structure and of the spatio-temporal noise correlation structures. We find that the short-term risk premia oscillates around zero, but becomes negative in the long run. We identify the Samuelson effect in the volatility term structure and volatility bumps, explained by market fundamentals. Furthermore we find evidence for coloured noise and correlated residuals, which we model by a Hilbert space-valued normal inverse Gaussian Lévy process with a suitable covariance functional.

**JEL Classification:** C02, C13, C23

**Keywords:** spatio-temporal models, price forward curves, term structure volatility, risk premia, electricity markets

---

\*Department of Mathematics, University of Oslo, PO Box 1053 Blindern, N-0316 Oslo, Norway, fredb@math.uio.no, Fax: +47 22 85 43 49.

<sup>†</sup>\*Corresponding author: Florentina Paraschiv, NTNU Business School, Norwegian University of Science and Technology, 7491 Trondheim, florentina.paraschiv@ntnu.no and University of St. Gallen, Institute for Operations Research and Computational Finance, Bodanstrasse 6, CH-9000 St. Gallen, Switzerland

# 1 Introduction

There exist two main approaches for modelling forward prices in commodity and energy markets. The classical way goes by specifying a stochastic model for the spot price, and from this model derive the dynamics of forward prices based on no-arbitrage principles (see Lucia and Schwartz (2002), Cartea and Figueroa (2005), Roncoroni and Geman (2006), Benth, Kallsen, and Meyer-Brandis (2007), Garcia, Klüppelberg, and Müller (2011), Barndorff-Nielsen, Benth, and Veraart (2013), Weron and Zator (2014), and Benth, Klüppelberg, Müller, and Vos (2014)). The alternative is to follow the Heath–Jarrow–Morton approach and to specify the dynamics of the forward prices directly, as it has been done in Roncoroni and Guiotto (2001), Benth and Koekebakker (2008), Weron and Borak (2008) and Kiesel, Schindlmayr, and Boerger (2009). All these studies model the forward prices using multifactor models driven by Brownian motion. However, empirical findings in Koekebakker and Ollmar (2005), Frestad (2008) suggest that there is a substantial amount of variation in forward prices which cannot be explained by a few common factors. Furthermore, the models that directly specify the dynamics of forward contracts ignore the fact that the returns of forward prices in electricity markets are far from being Gaussian distributed and have possible stochastic volatility effects.

The idea of modeling power forward prices with a random field model goes back to Audet, Heiskanen, Keppo, and Vehviläinen (2004), who studied theoretically a Gaussian model with certain mean-reversion characteristics. Their modelling framework is closely related to Kennedy (1994) and Goldstein (2000) who proposed random field models for the term structure of interest rates. Random-field models for forward prices in power markets have been explored statistically and mathematically by Andresen, Koekebakker, and Westgaard (2010). There the authors model electricity forwards returns for different times to maturity using a multivariate normal inverse Gaussian (NIG) distribution to capture the idiosyncratic risk and heavy tails behavior and conclude the superiority of this approach versus Gaussian-based multifactor models in terms of goodness of fit. Their

28 analysis seems to be based on the assumption that forward prices follow an exponential  
29 spatio-temporal stochastic process. When modeling forward prices evolving along time *to*  
30 maturity, the so-called Musiela parametrization, rather than time *at* maturity, one must  
31 be careful with how the time to maturity affects a price change. Indeed, in this so-called  
32 Musiela parametrization context of forward prices an additional drift term must be added  
33 to the dynamics to preserve arbitrage-freeness of the model. .

34 In this paper we propose to model the forward price dynamics by a spatio-temporal  
35 random field based on the Heath-Jarrow-Morton (HJM) approach under the Musiela  
36 parametrization (see Heath, Jarrow, and Morton (1992)), which ensures an arbitrage-  
37 free dynamics. After discretizing the model in time and space, we can separate seasonal  
38 features in the risk premium and random perturbations of the prices, and apply this to  
39 obtain information of the statistical characteristics of the data. Our model formulation  
40 disentangles typical components of forward prices such as: the deterministic seasonality  
41 pattern and the stochastic component including the market price of risk and the noise.  
42 We show the importance of rigourously modeling each component in the context of an  
43 empirical application to electricity forward prices, in which a unique panel data set of  
44 2'386 hourly price forward curves is employed for the German electricity index PHELIX.  
45 The index is generated each day for a horizon of 6 years, ranging from 01/01/2009 until  
46 15/07/2015. Each day a new price forward curve (PFC) is generated based on the newest  
47 information from current futures prices observed at EPEX.<sup>1</sup>

48 The dynamics of price forward curves (PFCs) are modeled with respect to two  
49 dimensions: temporal and spatial (the space dimension here refers to *time to maturity* of  
50 the forward). In particular, the changes in the level of a PFC for one specific maturity  
51 point between consecutive days reflect two features:

52 Firstly, as time passes, dynamics in time of on-going futures prices with a certain  
53 delivery period reflect changes in the market expectation. In particular, maturing futures

---

<sup>1</sup>Electricity for delivery on the next day is traded at the European Power Exchange (EPEX SPOT) in Paris.

54 are replaced by new ones in the market.<sup>2</sup> Changes in the market expectations reflect  
55 updates in weather forecasts, planned outages due to maintenance of power plants, en-  
56 ergy policy announcements or expected market structural changes. Germany adopted the  
57 Renewable Energy Act (EEG) in 2000, accordingly to which producers of renewable ener-  
58 gies (wind, photovoltaic etc.) receive a guaranteed compensation (technology dependent  
59 feed-in tariffs). Renewable energies are fed with priority into the grid, replacing thus in  
60 production other traditional fuels (oil, gas, coal). Given the difficulty of getting accurate  
61 weather forecasts, electricity demand/supply disequilibria became more frequent, which  
62 increased the volatility of electricity prices. Furthermore, it has been empirically shown  
63 that due to the low marginal production costs of wind and photovoltaic, the general level  
64 of electricity prices decreased over time (see Paraschiv, Erni, and Pietsch (2014)), which  
65 explains the shift in time of the general level of the analyzed PFCs.

66 Secondly, as time passes, the time to maturity of one specific product decreases and  
67 maturing futures are replaced by new ones in the market. In the German electricity mar-  
68 ket, weekly, monthly, quarterly and yearly futures are traded. Given the small number of  
69 different exchange-traded futures, and thus different maturities, the stochastic component  
70 of the (deseasonalized) PFCs shows a typical step-wise pattern when depicted graphically.  
71 Indeed, the different futures prices are represented as vertical lines over their respective  
72 delivery periods, with the height of the lines being the prices. Hence, the change in the  
73 level of the PFC over a time step is impacted through a change in the market expectations  
74 as well as a change in time to maturity. Both effects are displayed in Figure 1.

75 Our proposed model is fitted to the generated PFCs. We first perform a deseason-  
76 alization of the initial curves, where the seasonal component takes into account typical  
77 patterns observed in electricity prices (see Paraschiv (2013) and Paraschiv, Fleten, and  
78 Schürle (2015)). The stochastic component of the deseasonalized forward curves will  
79 consist of a risk premium and residual noise, where the risk premium is assumed to be

---

<sup>2</sup>In the German electricity market, weekly, monthly, quarterly or yearly futures are traded.

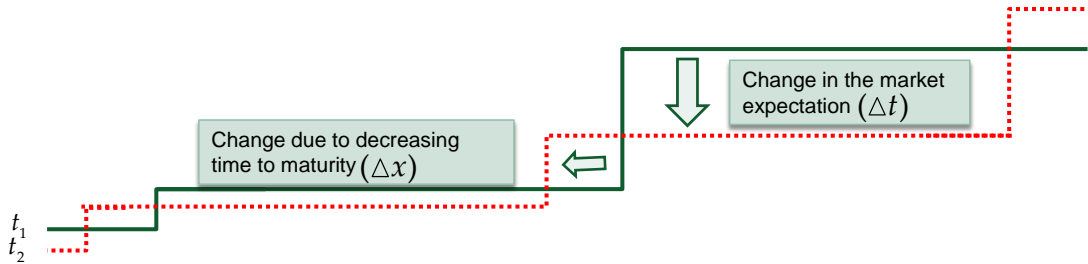


Figure 1: The effect of time and maturity change on the dynamics of forward prices.

80 proportional to the deseasonalized forward price by a term structure of market prices of  
 81 risk. We estimate the market price of risk and examine the distribution of the residual  
 82 noise volatility and its spatio-temporal correlations structures. Our results show that the  
 83 short-term risk premia oscillates around zero, but becomes negative in the long run, which  
 84 is consistent with the empirical literature (Burger, Graeber, and Schindlmayr (2007)). The  
 85 descriptive statistics of the noise marginals reveals clear evidence for a coloured-noise with  
 86 leptokurtic distribution and heavy-tails, which we suggest to model by a normal inverse  
 87 Gaussian distribution (NIG).<sup>3</sup> We further examine the term structure of volatility where  
 88 we are able to identify the Samuelson effect and volatility bumps. The occurrence of  
 89 volatility bumps are explained by the trading activity in the market for futures of specific  
 90 maturities (delivery periods). The spatial correlation structure of the noise is station-  
 91 ary with a fast-decaying pattern: decreasing correlations with increased distance between  
 92 maturity points along one curve.

93 Based on the empirical evidence, we further stylize our model and specify a spatio-  
 94 temporal mathematical formulation for the coloured noise time series. After explaining the  
 95 Samuelson effect in the volatility term structure, the residuals are modeled by a NIG Lévy

<sup>3</sup>Similar results can be found in Frestad, Benth, and Koekebakker (2010), who analyzed the distribution of daily log returns of individual forward contracts at Nord Pool and found that the univariate NIG distribution performed best in fitting the return data.

96 process with values in a convenient Hilbert space, which allows for a natural formulation  
97 of a covariance functional. We model, in this way, the typical fat tails and fast-decaying  
98 pattern of spatial correlations. Our modeling approach contributes in several ways beyond  
99 that of Andresen, Koekebakker, and Westgaard (2010): we disentangle the temporal from  
100 spatial (maturity) effects on the dynamics of forward prices honouring the no-arbitrage  
101 condition. This provides us with a data set in time and space where we can reveal and  
102 analyse the statistical properties of risk premia, of the noise volatility term structure and of  
103 the spatio-temporal noise correlation structures. Moreover, we introduce a mathematical  
104 framework for modelling the forward price dynamics which links to the empirics, including  
105 the Samuelson effect, the correlation structure along maturities and non-Gaussian price  
106 residuals. In conclusion, we formulate an arbitrage-free random field model for the power  
107 forward price dynamics in space and time which honours the statistical findings.

108 A mathematical treatise of the more general random field models of HJM type  
109 as we propose in this paper can be found in Benth and Krühner (2014). The issue  
110 of pricing derivatives for such random field models is discussed in Benth and Krühner  
111 (2015), while Benth and Lempa (2014) analyse portfolio strategies in energy markets  
112 with infinite dimensional noise. Our proposed forward price dynamics is thus suitable for  
113 further applications to both derivatives pricing and risk management. Efficient numerical  
114 approaches for simulation are also available, see for example Barth and Benth (2014).  
115 Thus, exotic energy derivatives may be priced by Monte Carlo simulations from the model.  
116 One may also simulate scenarios for hedges and portfolio positions in energy forwards. The  
117 flexibility and practical applicability of our proposed space-time random field dynamics  
118 makes it accessible for stress testing with other, competing models. For example, many  
119 in-house forward price models are based on multi-factor spot price dynamics. One may  
120 compare investment decisions in the two models, as well as analyse robustness of valuation  
121 of derivatives prices. Ambit fields is an alternative class of random fields which can be used  
122 for dynamic modeling of forward prices in power markets, see Barndorff-Nielsen, Benth,

123 and Veraart (2014). In Barndorff-Nielsen, Benth, and Veraart (2015) and Benth and  
124 Krühner (2015), infinite-dimensional cross-commodity forward price models are proposed  
125 and analysed.

126 The rest of the paper is organized as follows: In section 2 we present the mathe-  
127 matical formulation of the spatio-temporal random field model. In sections 3 and 4 we  
128 describe the data used for the application and present descriptive statistics on the risk  
129 premia, volatility, correlations and noise. The estimation results are shown in section 5,  
130 and in section 6 we specify a mathematical model for the residuals based on the statistical  
131 findings. Finally, section 7 concludes.

## 132 **2 Spatio-temporal random field modeling of forward** 133 **prices**

134 The Heath-Jarrow-Morton (HJM) approach (see Heath, Jarrow, and Morton (1992)) has  
135 been advocated as an attractive modelling framework for energy and commodity for-  
136 ward prices (see Benth, Šaltytė Benth, and Koekebakker (2008), Benth and Krühner  
137 (2014), Benth and Krühner (2015), Benth and Koekebakker (2008), Clewlow and Strick-  
138 land (2000)). If  $F_t(T)$  denotes the forward price at time  $t \geq 0$  for delivery of a commodity  
139 at time  $T \geq t$ , we introduce the so-called Musiela parametrization  $x = T - t$  and let  
140  $G_t(x)$  be the forward price for a contract with time to maturity  $x \geq 0$ . The graphical  
141 representation in Figure 2 shows comparatively the difference between thinking in terms  
142 of “time at maturity”,  $T$ , versus “time to maturity”  $x$ . Note that  $G_t(x) = F_t(t + x)$ .  
143 It is known (see e.g., Benth and Krühner (2014) and Benth and Krühner (2015)) that  
144 the stochastic process  $t \mapsto G_t(x)$ ,  $t \geq 0$  is the solution of a stochastic partial differential  
145 equation (SPDE),

$$dG_t(x) = (\partial_x G_t(x) + \beta(t, x)) dt + dW_t(x) \quad (1)$$

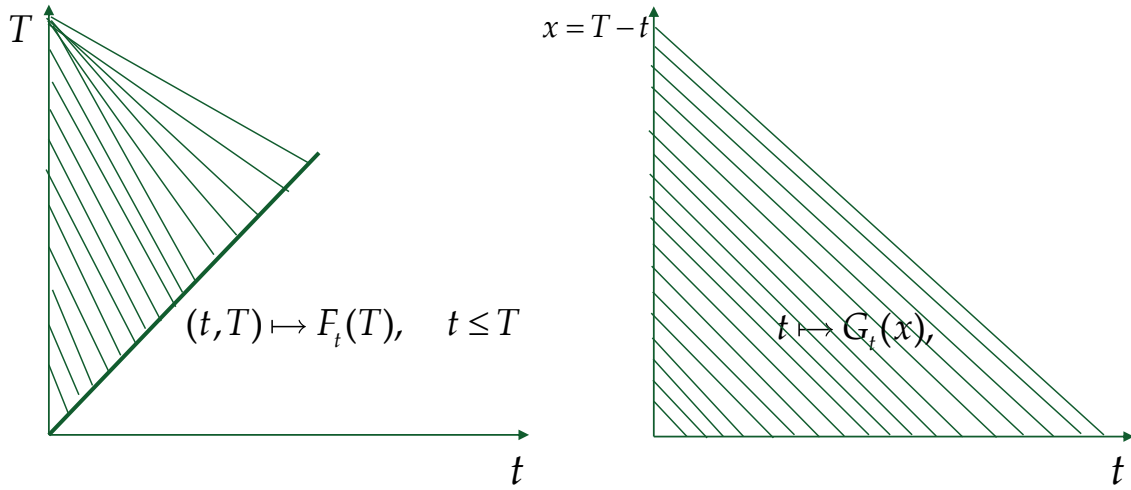


Figure 2: Theoretical model: time at maturity (first graph) versus time to maturity (second graph).

146 where  $\partial_x = \partial/\partial x$  is the differential operator with respect to time to maturity  $x$ ,  $\beta$  is  
 147 a spatio-temporal process modelling the market price of risk and finally  $W$  is a spatio-  
 148 temporal random field which describes the randomly evolving residuals in the dynamics.

149 To make the model for the forward price dynamics  $G$  rigorous, it has to be formulated  
 150 as a stochastic process in time, taking values in a space of curves on the positive real line  
 151  $\mathbb{R}_+$ . By a curve on  $\mathbb{R}_+$ , we understand the graph of a function  $x \mapsto f(x)$ , where  $x \in \mathbb{R}_+$ .  
 152 It would be more precise to talk of *functions* rather than *curves* on  $\mathbb{R}_+$ , but we want  
 153 to preserve the analogy to the frequently used notion of *forward curves*. Typically, this  
 154 space of curves is endowed with a Hilbert space structure. Denoting this Hilbert space  
 155 of curves by  $\mathcal{H}$ , the SPDE (1) is interpreted as a stochastic differential equation in  $\mathcal{H}$ .  
 156 Moreover, the  $\mathcal{H}$ -valued process  $W_t$  is a martingale, and encodes a correlation structure  
 157 in space and time for the forward prices, as well as the distribution of price increments  
 158 at fixed times to maturity  $x$  and the term structure of volatility. The latter includes  
 159 the Samuelson effect, which is predominant in commodity markets where stationarity of



160 prices is an empirical characteristic. We refer to Benth and Krühner (2015) for a rigorous  
 161 mathematical description and analysis of (1) in the Hilbert space framework, where a  
 162 specific example of an appropriate space of curves  $\mathcal{H}$  suitable for commodity markets is  
 163 proposed.

164 In this paper we will analyse a discrete-time version of the process  $G_t$ , obtained  
 165 from an Euler discretization of (1). In particular, our focus will be on an analysis of the  
 166 seasonal structure, the market price of risk and finally the probabilistic features of the  
 167 noise component  $W_t$ . To this end, suppose that

$$G_t(x) = f_t(x) + s_t(x), \quad (2)$$

168 where  $s_t(x)$  is a deterministic seasonality function. We assume that  $\mathbb{R}_+^2 \ni (t, x) \mapsto s_t(x) \in$   
 169  $\mathbb{R}$  is a bounded and measurable function, typically positive. Note that if we construct  
 170 the seasonality function from a spot price model, then naturally  $s_t(x) = s(t + x)$ , where  
 171  $s$  is the seasonality function of the commodity spot price (see Benth, Šaltytė Benth, and  
 172 Koekebakker (2008)). Indeed, it is reasonable that a seasonality function should depend  
 173 on the actual maturity date (i.e.,  $t + x = T$ ), which points to a specification where  
 174  $s_t(x) := s(t + x)$  also in the general case. Motivated by (1), we furthermore assume that  
 175 the deseasonalized forward price curve, denoted by  $f_t(x)$ , has the dynamics

$$df_t(x) = (\partial_x f_t(x) + \theta(x)f_t(x)) dt + dW_t(x), \quad (3)$$

with  $\mathbb{R}_+ \ni x \mapsto \theta(x) \in \mathbb{R}$  is a bounded and measurable function modeling the risk  
 premium. Hence, we suppose that the risk premium is proportional to the deseasonalized  
 forward price, with proportionality varying with time to maturity. With this definition,

we note that:

$$\begin{aligned}
dG_t(x) &= df_t(x) + ds_t(x) \\
&= (\partial_x f_t(x) + \theta(x)f_t(x)) dt + \partial_t s_t(x) dt + dW_t(x) \\
&= (\partial_x G_t(x) + (\partial_t s_t(x) - \partial_x s_t(x)) + \theta(x)(G_t(x) - s_t(x))) dt + dW_t(x).
\end{aligned}$$

176 As indicated above, naturally  $s_t(x) = s(t+x)$ , and hence  $\partial_t s_t(x) = \partial_x s_t(x)$ . Therefore, we  
177 see that  $G_t(x)$  satisfies (1) with  $\beta(t, x) := \theta(x)f_t(x)$ , i.e., that the market price of risk is  
178 proportional to the deseasonalized forward prices. Note that we have implicitly assumed  
179 differentiability of  $s_t(x)$  in the above derivation.

Let us next discretize the dynamics of  $f_t$  in (3), in order to obtain a time series dynamics of the (deseasonalized) forward price curve. Let  $\{x_1, \dots, x_N\}$  be a set of equidistant time-to-maturity dates with resolution  $\Delta x := x_i - x_{i-1}$  for  $i = 2, \dots, N$ . At time  $t = \Delta t, \dots, M\Delta t$ , where  $M\Delta t = T$  for some terminal time  $T$ , we observe for each time-to-maturity date  $x \in \{x_1, \dots, x_N\}$  a point on the price-forward curve  $G_t(x)$  and a corresponding point on the seasonality curve  $s_t(x)$ . A standard approximation of the derivative operator  $\partial_x$  is

$$\partial_x f_t(x) \approx \frac{f_t(x + \Delta x) - f_t(x)}{\Delta x}$$

180 Next, after doing an Euler discretization in time of (3), we obtain the time series approx-  
181 imation for  $f_t(x)$ . With  $x \in \{x_1, \dots, x_N\}$  and  $t = \Delta t, \dots, (M-1)\Delta t$ ,

$$f_{t+\Delta t}(x) = (f_t(x) + \frac{\Delta t}{\Delta x}(f_t(x + \Delta x) - f_t(x)) + \theta(x)f_t(x)\Delta t + \epsilon_t(x)) \quad (4)$$

182 where  $\epsilon_t(x) := W_{t+\Delta t}(x) - W_t(x)$ . We define the time series  $Z_t(x)$  for  $x \in \{x_1, \dots, x_N\}$   
183 and  $t = \Delta t, \dots, (M-1)\Delta t$ ,

$$Z_t(x) := f_{t+\Delta t}(x) - f_t(x) - \frac{\Delta t}{\Delta x}(f_t(x + \Delta x) - f_t(x)) \quad (5)$$

184 which implies

$$Z_t(x) = \theta(x)f_t(x)\Delta t + \epsilon_t(x), \quad (6)$$

185 where changes between the stochastic components of forward curves incorporate risk pre-  
186 mia and changes in the noise. Since we are interested in analysing the properties of the  
187 noise volatility, to account for Samuelson effect in forward prices, the model residuals  
188  $\epsilon_t(x)$  are further decomposed in:

$$\epsilon_t(x) = \sigma(x)\tilde{\epsilon}_t(x) \quad (7)$$

189 where  $\tilde{\epsilon}_t(x)$  are the standardized residuals.

190 The time series model (6) will be our object of study in this paper, where we are  
191 concerned with inference of the market price of risk proportionality factor  $\theta(x)$  and the  
192 probabilistic structure of  $\tilde{\epsilon}_t(x)$ . Since our concern is power markets, we aim at a (time and  
193 space) discrete curve  $Z_t(x)$  from forward prices over a delivery period. How to recover  
194 data for  $Z$  in such markets will be discussed in the next section. We remark here that we  
195 will choose a procedure of constructing a seasonal function which provides information  
196 on  $s_t(x)$  at discrete time and space points. By smooth interpolation, we may assume that  
197  $\partial_t s_t(x) = \partial_x s_t(x)$ .

### 198 **3 Generation of Price Forward Curves: theoretical** 199 **background**

200 In our empirical analysis we employed a unique data set of hourly price forward curves  
201 (HPFC)  $G_t(x_1), \dots, G_t(x_N)$  generated each day between 01/01/2009 and 15/07/2015  
202 based on the latest information from the observed futures prices for the German elec-  
203 tricity Phelix price index. We choose the distance between the maturity points to be  
204  $\Delta x = 1day$ , but will also in some instances consider longer maturity time steps in our

205 analysis. However, unless otherwise explicated,  $\Delta x = 1day$  is the choice. In this section  
 206 we describe how these curves were produced from market prices.

207 For the derivation of the HPFCs we follow the approach introduced by Fleten and  
 208 Lemming (2003). At any given time the observed term structure at EEX is based only on  
 209 a limited number of traded futures/forward products. Hence, a theoretical hourly price  
 210 curve, representing forwards for individual hours, is very useful but must be constructed  
 211 using additional information. We model the hourly price curve by combining the infor-  
 212 mation contained in the observed bid and ask prices with information about the shape of  
 213 the seasonal variation.

214 Recall that  $G_t(x)$  is the price of the forward contract with time to maturity  $x$ ,  
 215 where time is measured in hours, and let  $F_t(T_1, T_2)$  be the settlement price at time  $t$  of a  
 216 forward contract with delivery in the interval  $[T_1, T_2]$ . The forward prices of the derived  
 217 curve should match the observed settlement price of the traded futures product for the  
 218 corresponding delivery period, that is:

$$\frac{1}{\sum_{\tau=T_1}^{T_2} \exp(-r\tau/a)} \sum_{\tau=T_1}^{T_2} \exp(-r\tau/a) G_t(\tau - t) = F_t(T_1, T_2) \quad (8)$$

219 where  $r$  is the continuously compounded rate for discounting per annum and  $a$  is the num-  
 220 ber of hours per year. A realistic price forward curve should capture information about  
 221 the hourly seasonality pattern of electricity prices. For the derivation of the seasonality  
 222 shape of electricity prices we follow Paraschiv (2013) and Paraschiv, Fleten, and Schürle  
 223 (2015). Basically we fit the HPFC to the seasonality shape by minimizing

$$\min \left[ \sum_{x=1}^N (G_t(x) - s_t(x))^2 \right] \quad (9)$$

224

225 subject to constraints of the type given in equation (8) for all observed instruments, where

226  $s_t$  is the hourly seasonality curve (we refer to Fleten and Lemming (2003) for details).<sup>4</sup>  
227 We offer a detailed description of the methodology used to derive the seasonality shape  
228 for the Phelix electricity prices in the internet appendix A. To keep the optimization  
229 problem feasible, we follow the standard procedure (see Benth, Koekebakker, and Ollmar  
230 (2007)) to remove overlapping contracts as well as contracts with delivery periods which  
231 are completely overlapped by other contracts with shorter delivery periods. From no-  
232 arbitrage relationships (see Benth, Šaltytė Benth, and Koekebakker (2008, Eq. (6.6) on  
233 p. 165)), there is no information loss in removing a futures contract with delivery period  
234 that is overlapped by one or more other futures contracts.

235 An alternative approach to extract power forward curves from a discrete set of  
236 traded contract using spline interpolation is suggested by Benth, Koekebakker, and Ollmar  
237 (2007). Recently, Caldana, Fusai, and Roncoroni (2016) proposed a method combining  
238 non-parametric filtering with convex interpolation.

## 239 4 Empirical analysis

240 The original input to our analysis are 2'386 hourly price forward curves for PHELIX,  
241 the German electricity index, generated each day between 01/01/2009 and 15/07/2015,  
242 for a horizon of 5 years. The curves have been provided by the Institute of Operations  
243 Research and Computational Finance, University of St. Gallen and have been generated  
244 consistently based on the approach described in section 3. In a first step, we eliminated  
245 the deterministic component of the hourly price forward curves, as shown in Equation  
246 (2). To keep the analysis tractable, we chose to work with daily, instead of hourly curves.  
247 Thus, the stochastic component of each hourly price forward curve,  $f_t(x)$ , has been filtered

---

<sup>4</sup>In the original model, Fleten and Lemming (2003) applied, for daily time steps, a smoothing factor to prevent large jumps in the forward curve. However, in the case of hourly price forward curves, Bloechlinger (2008) (p. 154) concludes that the higher the relative weight of the smoothing term, the more the hourly structure disappears. We want that our HPFC reflects the hourly pattern of electricity prices and therefore in this study we have set the smoothing term in Fleten and Lemming (2003) to 0.

248 out for hour 12 of each day over a horizon of 2 years.<sup>5</sup> The choice of hour 12 is intuitive,  
249 since it has been empirically shown that over noon electricity prices are more volatile,  
250 due to the increase in the infeed from renewable energies over the last years in Germany  
251 (Paraschiv, Erni, and Pietsch (2014)). It is interesting, therefore, to analyse the volatility  
252 of the noise  $\epsilon_t(x)$  (Equation (6)) for this particular traded product.

253 We analyse the stochastic component of price forward curves and examine further  
254 the market price of risk, the distribution of the noise volatility and its spatio-temporal  
255 correlations structures. In the internet appendix B we show a more detailed analysis  
256 of the stochastic component of PFCs including a visual inspection and discuss the eco-  
257 nomical background of fundamental variables which determined changes in the stochastic  
258 component over time.

## 259 4.1 Analysis of the risk premium

260 In the case of storable commodities, arbitrage-based arguments imply that the forward  
261 price is equal to the spot price times discount factors involving the risk-free interest rate,  
262 storage costs and the convenience yield (see Geman (2005)). However, electricity is non-  
263 storable, so this link does not exist here. Therefore, it can be expected that forward prices  
264 are formed as the sum of the expected spot price plus a risk premium that is paid by risk-  
265 averse market participants for the elimination of price risk. We estimated Equation (6)  
266 for each time-series  $Z_t(x)$  and  $f_t(x)$ ,  $t \in \{1, \dots, T\}$  of each point  $x \in \{x_1, \dots, x_N\}$ . For  
267 taking  $\Delta t = 1 \text{ day}$  and  $\Delta x = 1 \text{ day}$ , the estimated risk premia will be a  $(1 \times (N - 1))$   
268 vector. Estimation results are shown in Figure 3.

269 We observe that the risk premia take values between a minimum of  $-0.086$  and  
270 maximum  $0.017$ . They oscillate around zero and have a higher volatility over the first  
271 three quarters of the year along the curve, so for shorter time to maturities. However,

---

<sup>5</sup>For the generation of PFCs on horizons longer than 2 years, only yearly futures are still observed, so the information about the market expectation becomes more general. We therefore decided to keep the analysis compact and analyse 2 years long truncated curves.

272 on the medium/long-run the risk premia are predominantly negative and their volatility  
273 seems to stabilize for the second year.

274 The finding that the short-term risk premia oscillate around zero is consistent with  
275 the findings in the literature. For example Pietz (2009) found that the risk premium  
276 may be positive or negative, depending on the average risk aversion in the market. It  
277 may vary in magnitude and sign throughout the day and between seasons. Furthermore,  
278 Paraschiv, Fleten, and Schürle (2015) found that short-term risk premia are positive  
279 during the week and decrease or become negative for the weekend. The disentangled  
280 pattern of risk premia between seasons, working/weekend days cannot be investigated  
281 here directly, though, since we used for the estimation a time-series of each point along  
282 one curve, making use of all generated PFCs used as input. We are in fact interested  
283 to examine the evolution of risk premia with increasing time to maturity. In the long-  
284 run, the negative risk premia confirm previous findings in the literature (see e.g., Burger,  
285 Graeber, and Schindlmayr (2007)): producers accept lower futures prices, as they need  
286 to make sure that their investment costs are covered.

## 287 **4.2 Analysis of term structure volatility**

288 In Figure 4 we plot the term structure volatility  $\sigma(x)$ , for  $x \in \{x_1, \dots, x_N\}$ , as defined  
289 in Equation (7). Overall we observe that the volatility decreases with increasing time  
290 to maturity. In particular, it decays faster for shorter time to maturity and it shows a  
291 bump around the maturity of 1 month. Around the second (front) quarter the volatility  
292 starts increasing again, showing a second bump around the third quarter. The reason is  
293 that for time to maturities longer than one month, in most of the cases weekly futures  
294 are not available anymore, so the next shortest maturity available in the market is the  
295 front month future. That means: if market participants are interested in one sub-delivery  
296 period within the second month, there are no weekly futures available to properly price  
297 their contracts, but the only available information is from the front month futures price.

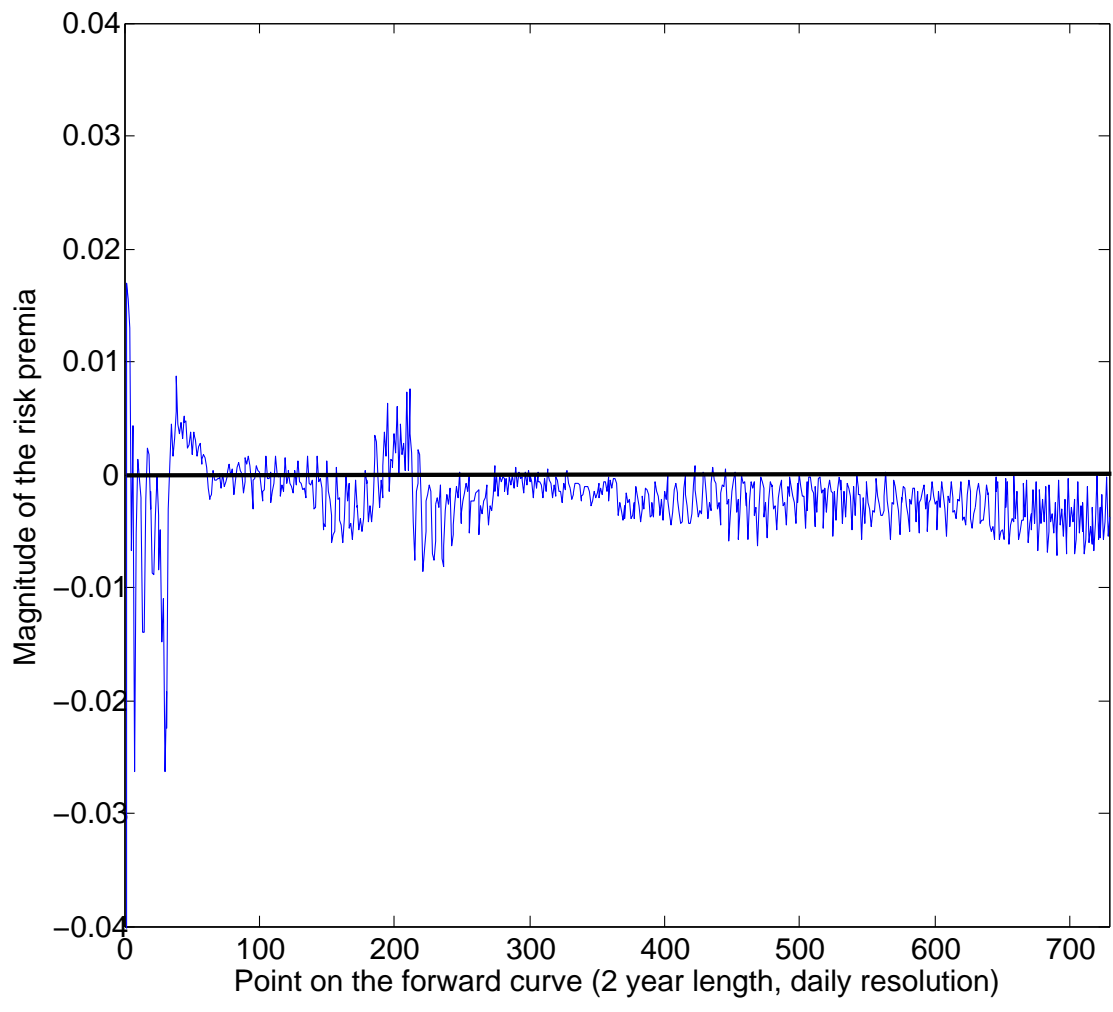


Figure 3: Risk premia along one curve (2-year length, daily resolution)



298 It is known that the volume of trades for this front month future increases, thus inducing a  
 299 higher volatility of the corresponding forward prices. In Figure 5 we observe that indeed,  
 300 the front month future has the highest and the most volatile volume of trades over the  
 301 investigated time period, compared to the other monthly traded contracts. A similar  
 302 effect is around the front quarter, when monthly futures are not observed anymore, but  
 303 the information about the level of the (expected) price is given by the corresponding  
 304 quarterly future contract. In consequence, the volume of trades for the front quarterly  
 305 future and for the 2nd available quarterly future increases, these being the most traded  
 306 products in the market, as shown in Figure 6. This explains the increase in the volatility  
 307 during the front quarter segment of the forward curve and the second bump.

308 The jigsaw pattern of the volatility curve reflects the weekend effect: the volatility  
 309 of forwards is lower during weekend versus working days. A similar pattern is observed  
 310 in the spot price evolution, as shown in Paraschiv, Fleten, and Schürle (2015).

### 311 4.3 Statistical properties of the noise time series

312 The analysis of the noise time-series  $\tilde{\epsilon}_t$  (see Equation (7)) is twofold: First, we examine  
 313 the statistical properties of individual time series  $\tilde{\epsilon}_t(x_i)$  and in particular we check for  
 314 stationarity, autocorrelation and ARCH/GARCH effects. Secondly, we examine patterns  
 315 in the correlation matrix with respect to the time/maturity dimensions. Thus, we are  
 316 interested in the correlations between  $\tilde{\epsilon}_t(x_i)$  and  $\tilde{\epsilon}_t(x_j)$ , for  $i, j \in \{1, \dots, N\}$ ,  $t = 1, \dots, T$   
 317 to examine the effect of the time to maturity on the joint dynamics between the noise  
 318 components. Furthermore, we are interested in the correlations between noise curves,  
 319 with respect to the points in time where these have been generated: correlations be-  
 320 tween  $\tilde{\epsilon}_m(x_1), \dots, \tilde{\epsilon}_m(x_N)$  and  $\tilde{\epsilon}_n(x_1), \dots, \tilde{\epsilon}_n(x_N)$ , for  $m, n \in \{1, \dots, T\}$ . The analysis is  
 321 performed initially for taking  $\Delta x = 1day$  and  $\Delta t = 1day$ , as defined in Equation (5).

322 We are further interested to see whether the statistical properties of the noise as  
 323 well as the correlations between its components change, if we vary the maturity step

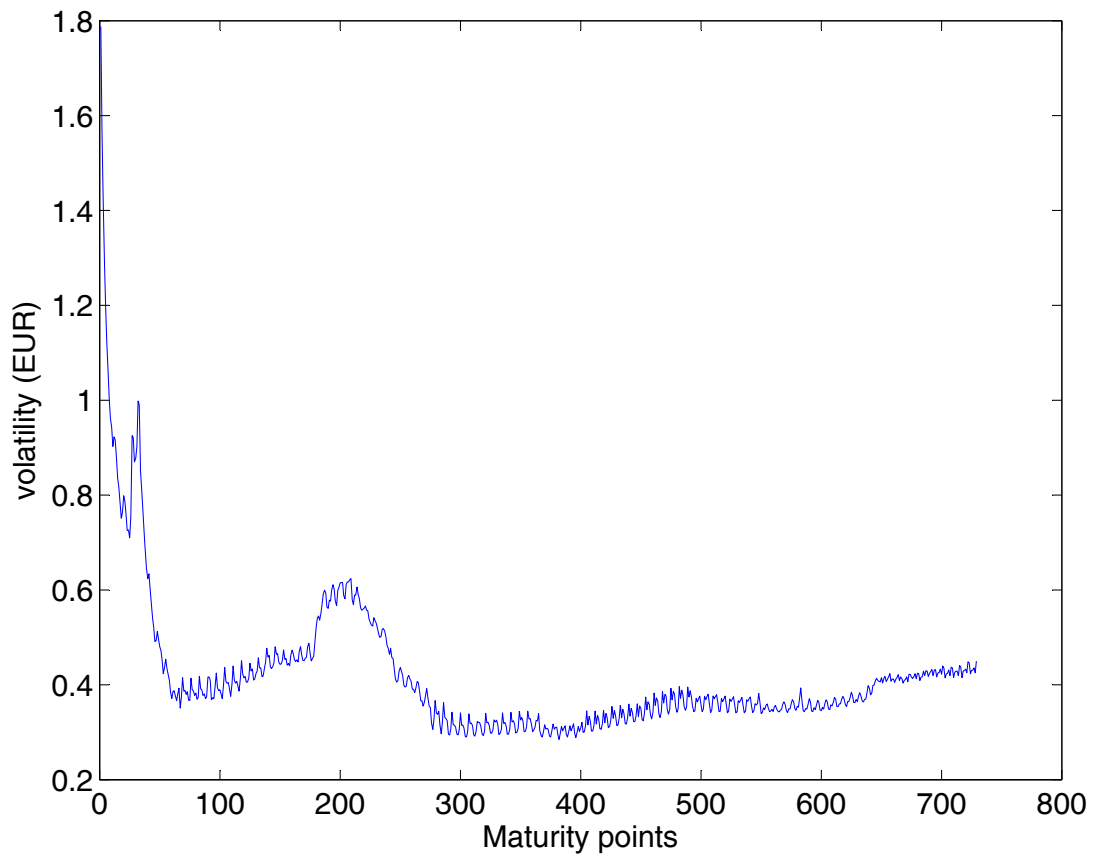


Figure 4: The empirical volatility term structure

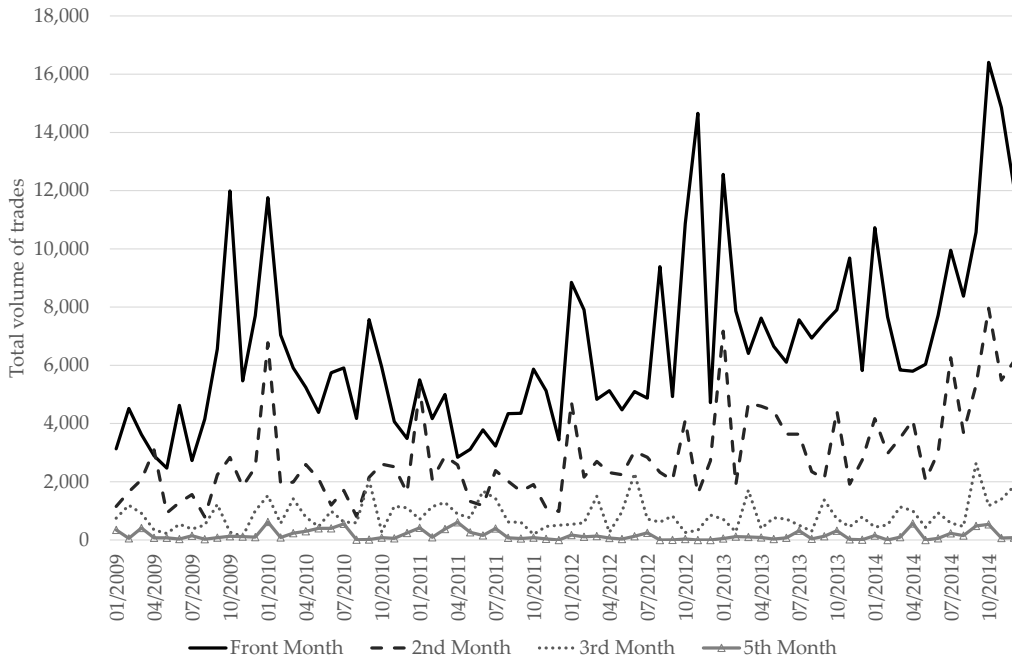


Figure 5: The sum of traded contracts for the monthly futures at EPEX (own calculations, source of data: [ems.eex.com](http://ems.eex.com)).

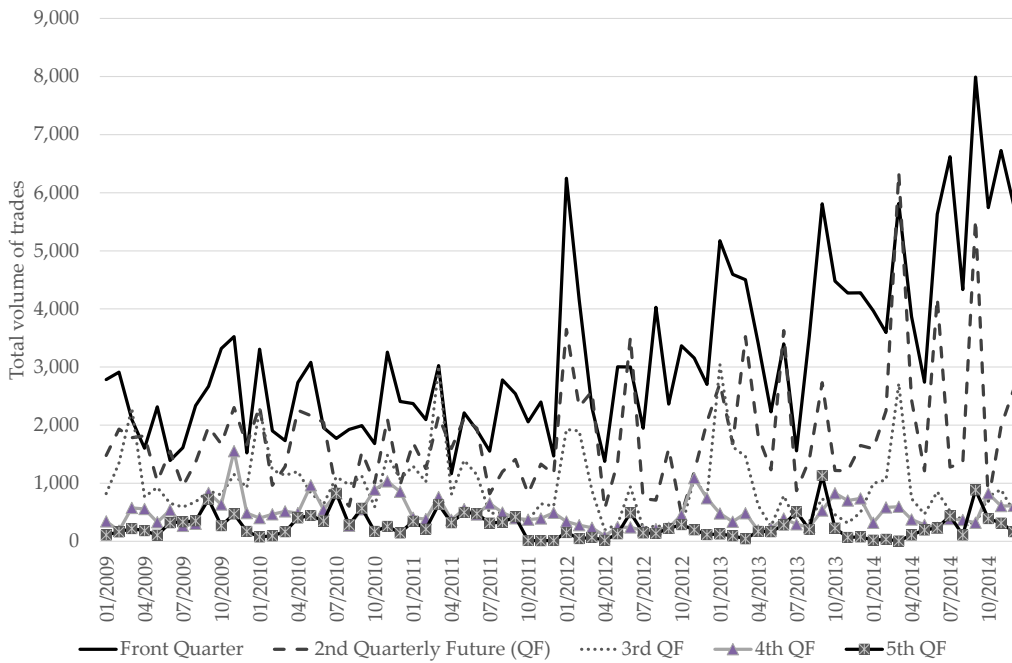


Figure 6: The sum of traded contracts for the quarterly futures at EPEX (own calculations, source of data: [ems.eex.com](http://ems.eex.com)).

324  $\Delta x$  in Equation (5) (and implicitly  $\Delta t$ ). When changing  $\Delta x$ , we are also changing the  
 325 numerical differentiation in Equation (5) with respect to  $x$ , and in particular the range  
 326 (in the maturity direction) for when information is accounted for. Various maturity  
 327 steps may lead to slightly different properties of the noise, given the stepwise pattern  
 328 of the deaseasonalized price forward curves  $f_t(x)$ , as shown in Figures 1 and 2 in the  
 329 internet appendix B. The stepwise pattern comes from the different level of futures prices  
 330 of different maturities taken as input for the generation of price forward curves. Futures  
 331 have different delivery periods, weekly, monthly, quarterly, yearly, and at each point when  
 332 a new future is observed, the level in the generated price forward curve changes (recall  
 333 Figure 1). As the choice of  $\Delta x$  dictates when information from observed futures contracts  
 334 is accounted for, it will impact the generated price forward curve. This is taken over in  
 335 the stochastic component  $f_t(x)$ . Furthermore, within one week, we observe the weekend  
 336 effect: the price level is different between working/weekend days. All these cause sparse  
 337 matrices in the noise, given the many values of “zero” obtained after differentiating.

338 To assess the impact of stepwise changes in the stochastic component of price for-  
 339 ward curves  $f_t(x)$ , we replicated the analysis for one additional case study: We further  
 340 investigated the effect of a change between consecutive weekly futures prices by taking  
 341  $\Delta x = 7days$ . This choice of maturity step further affects the impact from monthly and  
 342 quarterly products on the level of the generated curve.

### 343 4.3.1 Stationarity, Autocorrelation, ARCH/GARCH effects

344 The stationarity, autocorrelation pattern and ARCH/GARCH effects are computed for  
 345 each case study of  $\Delta x/\Delta t$ , namely 1 day and 7 days shifts in maturity (and time). To  
 346 reduce the complexity, we compute these statistics for time series of equidistant points  
 347 along the curve’s length:  $\tilde{\epsilon}_t(x_k)$ , where  $k \in \{1, \dots, N\}$ . In choosing  $k$  we increment over  
 348 90 days (approximately one quarter) along one noise curve. To test for stationarity, we  
 349 applied the Augmented Dickey-Fuller (ADF) and Phillips-Perron tests for a unit root in

350 each univariate time series  $\tilde{\epsilon}_t(x_k)$ . Results are confirmed when applying the Kwiatkowski-  
 351 Phillips-Schmidt-Shin test statistic for stationarity (with intercept, no trend). Results are  
 352 available in Tables 1 and 2 for the case studies  $\Delta x = 1\text{day}$  and  $\Delta x = 7\text{days}$ , respectively.  
 353 For  $h = 0$ , we fail to reject the null that series are stationary. Unit root test results are  
 354 shown in detail in Table 3. Thus, all statistical tests conclude that time series  $\tilde{\epsilon}_t(x_k)$  are  
 355 stationary.

356 We further tested the hypothesis that the  $\tilde{\epsilon}_t(x_k)$  series are autocorrelated. Autocor-  
 357 relation test results are shown in Tables 1 and 2. We replicated the test for the level of  
 358 the noise time series and for their squared values (columns 2 and 3, respectively).  $h1 = 0$   
 359 indicates that there is not enough evidence to suggest that noise time series are autocor-  
 360 related. In Figures 7 and 8 we display the autocorrelation function for series  $\tilde{\epsilon}_t(x_k)$  for  
 361  $k \in \{90, 180, 270, 360\}$ , for the level and squared residuals, respectively. In the first case,  
 362 the pattern of the autocorrelation function for the level of residuals shows a typical white  
 363 noise pattern. Still, as expected, the autocorrelation function shows a slight decaying pat-  
 364 tern in the second case (Figure 8), where we look at the squared residuals. The decaying  
 365 pattern becomes more obvious when we move to the case study two, where the change in  
 366 maturity (and time) is set to 7 days, as shown in Figure 9. This is not surprising, since  
 367 an increment of maturity points and time of 7 days leads to less zero increments in the  
 368 noise time series overall, which allows a more visible pattern of autocorrelation. Results  
 369 of the autocorrelation test conclude our findings from the visual inspection: if in the basic  
 370 case study of  $\Delta x = 1\text{day}$  we did not find evidence for autocorrelation in all time series of  
 371 the noise (Table 1, second and third columns), there is clear evidence for autocorrelation  
 372 in all series with increasing maturity step  $\Delta x = 7\text{days}$ .

373 We further tested the hypothesis that there are significant ARCH effects in the  
 374  $\tilde{\epsilon}_t(x_k)$  series by employing the Ljung-Box Q-Test. Results are shown in the last columns  
 375 of Tables 1 and 2.  $h2 = 1$  indicates that there are significant ARCH effects in the noise  
 376 time-series. Independent of the maturity/time step chosen, time series are characterized

377 by ARCH effects, and thus by a volatility clustering pattern. In Equation (7) we filter  
 378 the volatility out of the marginal noise  $\epsilon_t(x)$ . However, the volatility is not time-varying  
 379 in our model, which explains that there is evidence for remaining stochastic volatility  
 380 (conditional heteroscedasticity) in the standardized residuals  $\tilde{\epsilon}_t(x)$ . We tested for a unit  
 381 root in the unobserved volatility process by testing for a unit root in the log of the squared  
 382 time series. Standard unit root tests (ADF, PP, KPSS) are known to suffer from extreme  
 383 size distortions in the presence of negative mean average (MA) roots which are expected  
 384 to occur, given the identified ARCH/GARCH results (see Wright (1999)). We therefore  
 385 apply the methodology in Perron and Ng (1996) who have proposed modified unit root  
 386 tests which are robust to large negative MA roots. As shown in Table 4, NG-Perron test  
 387 statistics show evidence for a unit root in the volatility process.

388 In the light of the identified ARCH/GARCH effects in the marginals  $\tilde{\epsilon}_t(x_k)$ , we  
 389 inspect their tail behavior by plotting the kernel smoothed empirical densities versus  
 390 normal distribution for series  $k \in \{1, 90, 180, 270\}$ , as shown in Figure 11. We observe  
 391 the strong leptokurtic pattern of heavy tailed marginals.

392 Overall we conclude that the model residuals are coloured noise, with heavy tails  
 393 (leptokurtic distribution) and with a tendency for conditional volatility.

### 394 4.3.2 Spatial Correlation

395 In the autocorrelation functions examined above, we show that there are temporal corre-  
 396 lations between forward curves produced at different points in time. In addition, we are  
 397 interested in the spatial correlation structure between  $\tilde{\epsilon}_t(x_i)$  and  $\tilde{\epsilon}_t(x_j)$ , for  $i, j \in 1, \dots, N$ ,  
 398 to examine how noise correlations change with increasing distance between the matu-  
 399 rity points along one curve. In Figure 10 we observe that correlations oscillate between  
 400 positive and negative, which is expected, given the nature of the (coloured) noise time  
 401 series (stationary, oscillating around 0). As expected, spatial correlations between matu-  
 402 rity points of up to 1 month (about 30 day) decay fast with increasing distance between

$\tilde{\epsilon}_t(x_k)$	Stationarity	Autocorrelation $\tilde{\epsilon}_t(x_k)$	Autocorrelation $\tilde{\epsilon}_t(x_k)^2$	ARCH/GARCH	
	h	h1	h1	h1	h2
Q0	0	1	1	1	1
Q1	0	0	0	0	0
Q2	0	1	1	1	1
Q3	0	0	0	1	1
Q4	0	1	1	0	0
Q5	0	1	1	1	1
Q6	0	1	1	1	1
Q7	0	1	1	1	1

Table 1: The time series are selected by quarterly increments (90 days) along the maturity points on one noise curve. Hypotheses tests results, case study 1:  $\Delta x = 1day$ . In column 'Stationarity', if  $h = 0$  we fail to reject the null that series are stationary. For 'Autocorrelation',  $h1 = 0$  indicates that there is not enough evidence to suggest that noise time series are autocorrelated. In the last column,  $h2 = 1$  indicates that there are significant ARCH effects in the noise time-series.

$\tilde{\epsilon}_t(x_k)$	Stationarity	Autocorrelation $\tilde{\epsilon}_t(x_k)$	Autocorrelation $\tilde{\epsilon}_t(x_k)^2$	ARCH/GARCH	
	h	h1	h1	h1	h2
Q0	0	1	1	1	1
Q1	0	1	1	1	1
Q2	0	1	1	1	1
Q3	0	1	1	1	1
Q4	0	1	1	1	1
Q5	0	1	1	1	1
Q6	0	1	1	1	1
Q7	0	1	1	1	1

Table 2: The time series are selected by quarterly increments (90 days) along the maturity points on one noise curve. Hypotheses tests results, case study 2:  $\Delta x = 7days$ . In column 'Stationarity', if  $h = 0$  we fail to reject the null that series are stationary. For 'Autocorrelation',  $h1 = 0$  indicates that there is not enough evidence to suggest that noise time series are autocorrelated. In the last column,  $h2 = 1$  indicates that there are significant ARCH effects in the noise time-series.

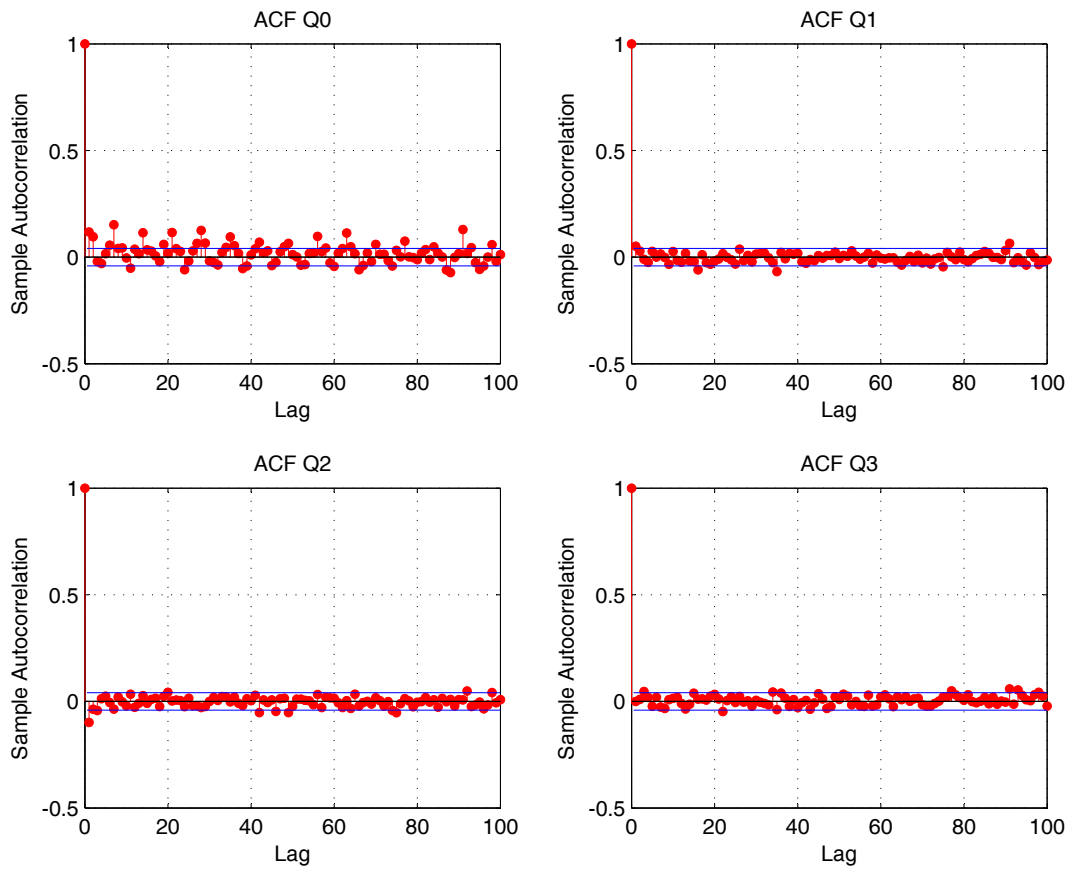


Figure 7: Autocorrelation function in the level of the noise time series  $\tilde{\epsilon}_t(x_k)$ , by taking  $k \in \{1, 90, 180, 270\}$ , case study 1:  $\Delta x = 1 \text{ day}$ .



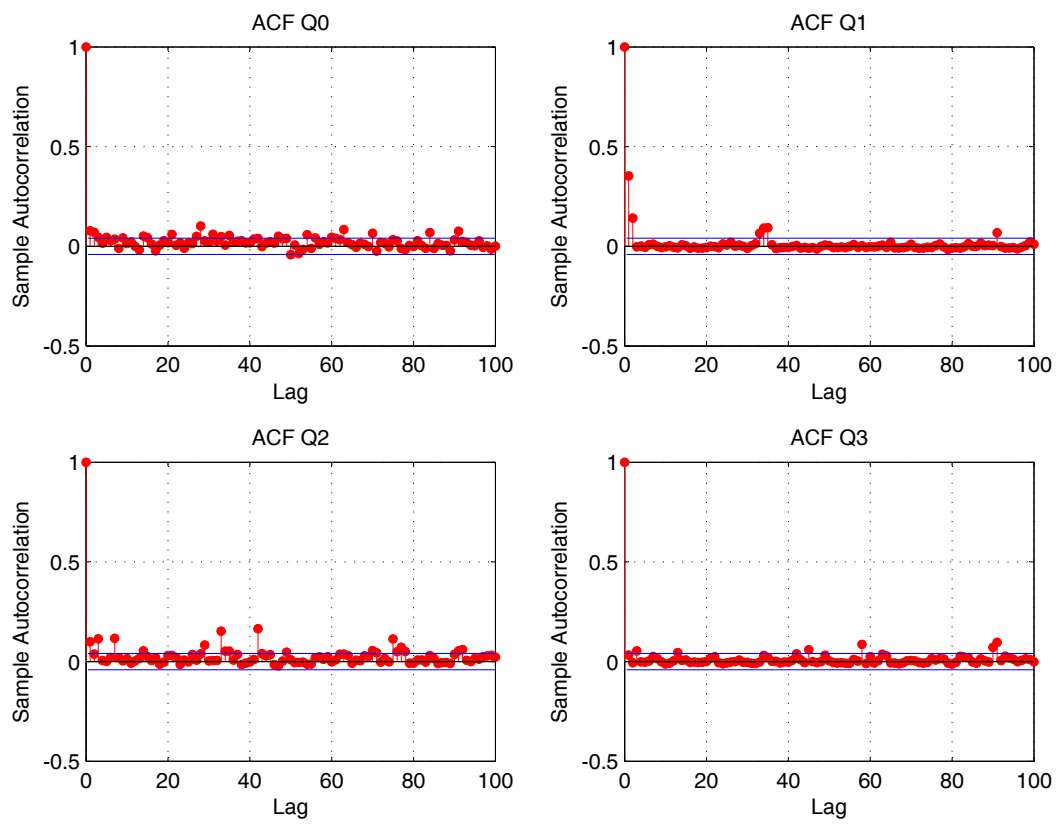


Figure 8: Autocorrelation function in the squared time series of the noise  $\tilde{\epsilon}_t(x_k)^2$ , by taking  $k \in \{1, 90, 180, 270\}$ , case study 1:  $\Delta x = 1 \text{ day}$ .

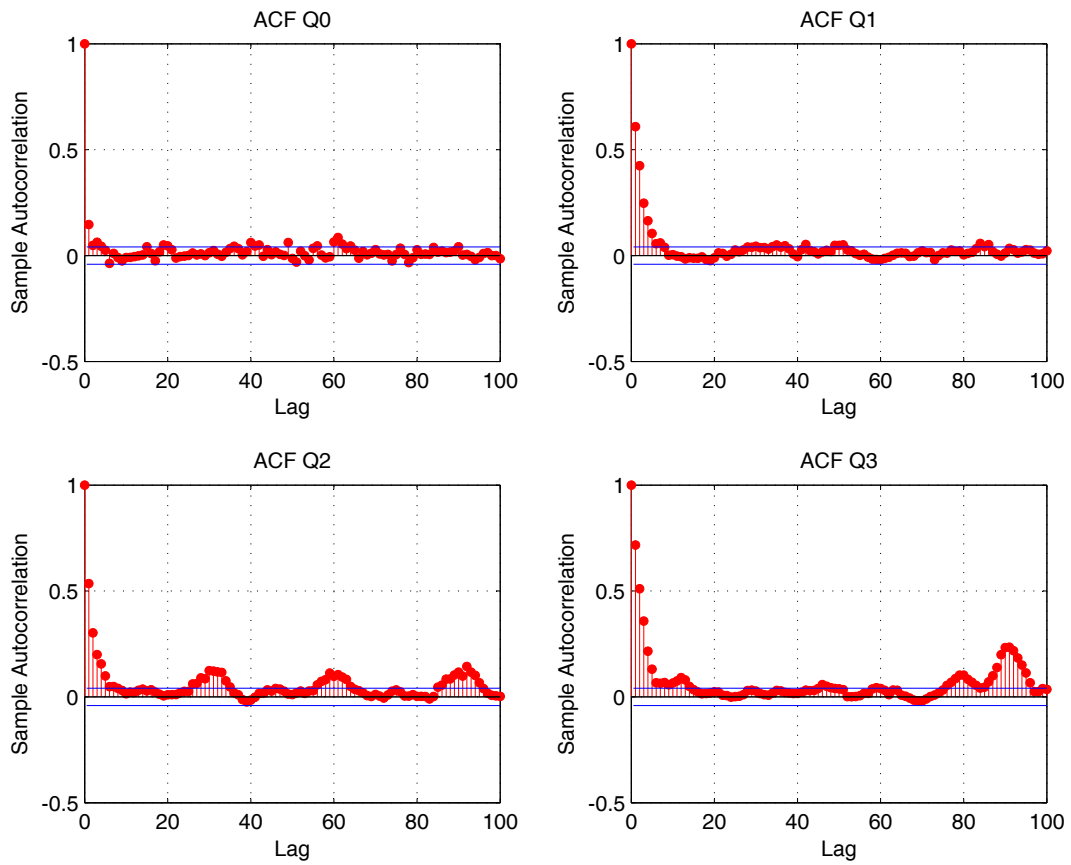


Figure 9: Autocorrelation function in the squared time series of the noise  $\tilde{\epsilon}_t(x_k)^2$ , by taking  $k \in \{1, 90, 180, 270\}$ , case study 2:  $\Delta x = 7 \text{ days}$ .

Test	Null hypothesis	Q0	Q1	Q2	Q3
ADF test	Unit root	-4.476*	-4.701*	-3.504*	-3.600*
PP test	Unit root	-52.550*	-51.755*	-52.623*	-52.720*
KPSS test	Stationarity	0.564	0.399	0.329	0.367

Table 3: *Unit root test results for series  $\tilde{\epsilon}_t(x_k)$  for quarterly increments in  $k \in 1, 90, 180, 270$ . Note: One star denotes significance at the 1% level. ADF refers to Augmented Dickey-Fuller test, PP to the Philips-Peron test and KPSS to the Kwiatkowski-Phillips-Schmidt-Shin test. The lag structure of the ADF test is selected automatically on the basis of the Bayesian Information Criterion (BIC). For PP and KPSS tests the bandwidth parameter is selected according to the approach suggested by Newey and West (1994).*

<b>NG-Perron test</b>	Q0	Q1	Q2	Q3
MZa	-2.457	-1.719	-1.901	-1.382
MZt	-0.967	-0.837	-0.891	-0.731

Table 4: *NG-Perron unit root test results for series  $\log(\tilde{\epsilon}_t(x_k)^2)$  for quarterly increments in  $k \in 1, 90, 180, 270$ . Note: We test the null hypothesis: series has a unit root. One star denotes significance at the 1% level. MZa and MZt are the three modified Z-test statistics of Perron and Ng (1996). The lag length of the NG-Perron test is selected automatically on the basis of the Spectral GLS-detrended AR based on Schwarz Information Criteria (SIC).*

403 them. This reflects the higher interest of market participants for maturing contracts. The  
404 correlations between maturity points situated at distances longer than 30 days are very  
405 low, oscillating around zero. However, correlations between 1 year distant maturity points  
406 slightly increase. This shows that the stochastic component of forward prices is driven by  
407 common factors at the same time of the year, which is reflected in a higher correlation  
408 between yearly futures products.

## 409 5 Modeling approach and estimation of the noise

410 Given the heavy tails of marginals identified in Figure 11, we model the noise marginals  
411  $\tilde{\epsilon}_t(x)$  by a Normal Inverse Gaussian distribution (NIG). The NIG distribution is a special  
412 case of the Generalized Hyperbolic Distribution for  $\lambda = -1/2$  and its density reads (see

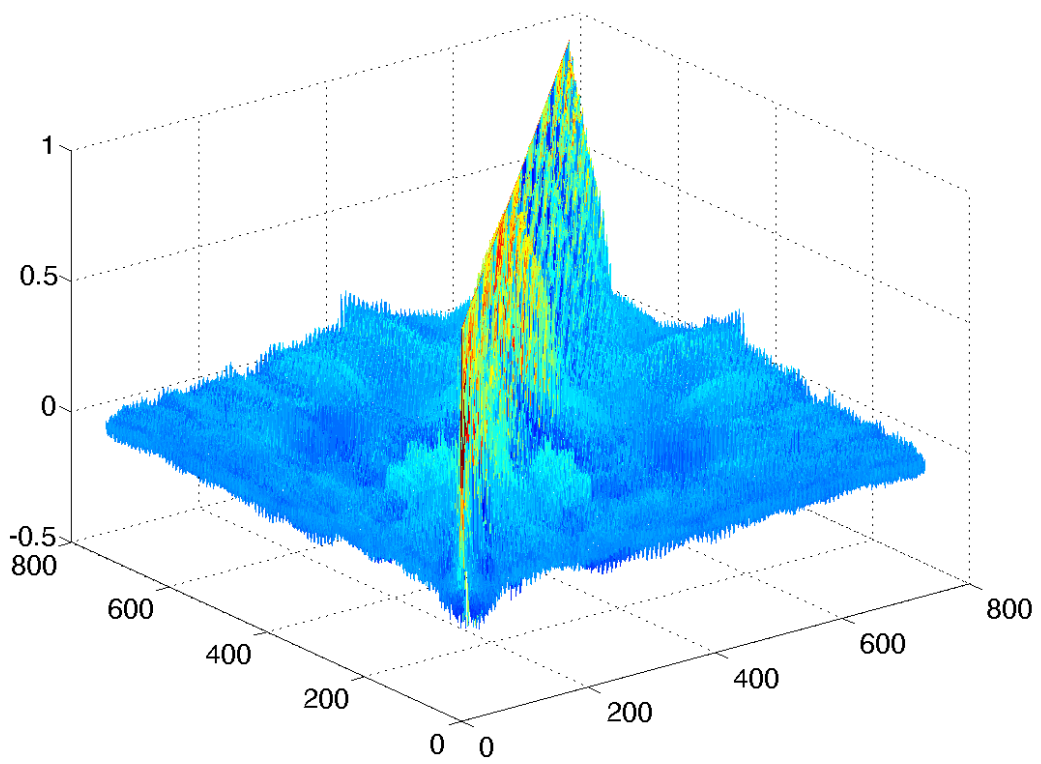


Figure 10: Correlation matrix with respect to different maturity points

Parameter	Q0	Q1	Q2	Q3
$\delta$	1.115 (0.102)	0.252 (0.007)	0.193 (0.005)	0.226 (0.006)
$\alpha$	1.083 (0.152)	0.188 (0.046)	0.116 (0.052)	0.195 (0.037)
$\beta$	0.111 (0.054)	-0.012 (0.024)	0.000 (0.022)	-0.001 (0.021)
$\mu$	-0.011 (0.049)	0.000 (0.004)	-0.004 (0.007)	-0.002 (0.007)

Table 5: Maximum likelihood estimates of NIG to  $\tilde{\epsilon}_t(x_k)$  by taking  $k \in \{1, 90, 180, 270\}$  for Q0,...,Q3, respectively.

Standard errors are shown in parentheses.

413 Benth, Šaltytė Benth, and Koekebakker (2008):

$$f_{NIG}(x) = \frac{\alpha}{\pi} \exp(\delta \sqrt{\alpha^2 - \beta^2} + \beta(x - \mu)) \frac{K_1(\alpha \delta \sqrt{1 + (\frac{x-\mu}{\delta})^2})}{\sqrt{1 + (\frac{x-\mu}{\delta})^2}} \quad (10)$$

414 We have firstly fitted a NIG by moment estimators. We observed that the fitted  
415 density performs visibly better than a normal distribution in explaining the leptokurtic  
416 pattern of time series. In a second step, we estimated NIG by maximum likelihood (ML).  
417 The mathematical formulation of the likelihood function and related gradients as input  
418 to the numerical optimization procedure are given in the internet appendix C.

419 The ML estimates improved further the fit of the NIG density. In Table 5 we show  
420 the ML estimates for the NIG distribution fitted to  $\tilde{\epsilon}_t(x_k)$  by taking  $k \in \{1, 90, 180, 270\}$ .  
421 In Figure 11 we show the kernel density estimates versus normal and the two versions  
422 of the NIG estimation. We confirm a realistic performance of the NIG distribution in  
423 explaining the heavy tail behavior of noise marginals.

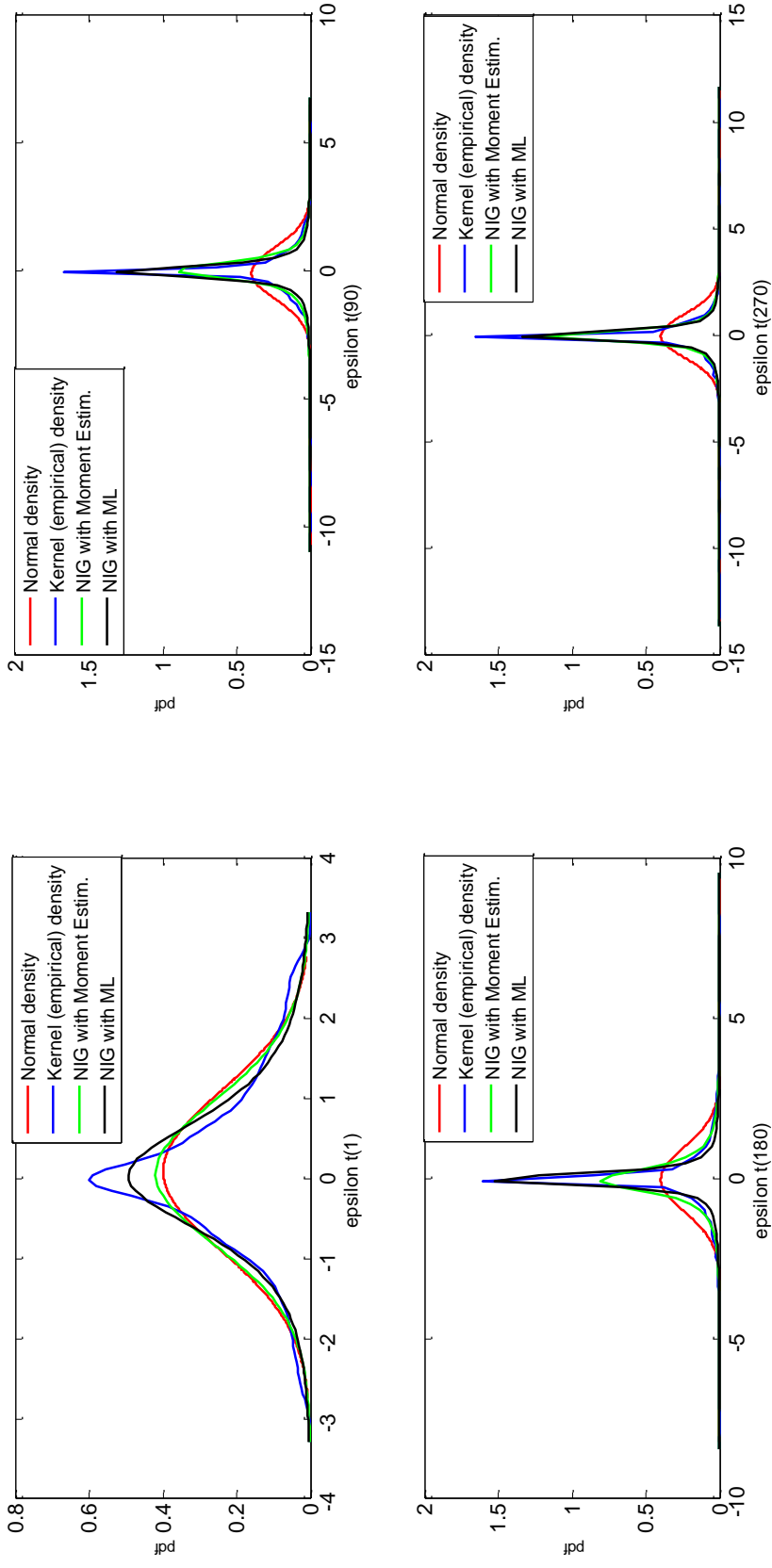


Figure 11: Density plots for  $\tilde{\epsilon}_t(x_k)$ , where  $k \in \{1, 90, 180, 270\}$ . The empirical density of the noise time series (blue) is compared to the densities of a normal distribution (red) and to the densities of a NIG distribution fitted to the data based on the moment estimates (green) and maximum likelihood (black)

## 6 Revisiting the spatio-temporal model of forward prices

In our empirical analysis of EPEX electricity forward prices, we have made use of a time series discretization of the deseasonalized term structure dynamics  $f_t(x)$  defined in (3). We have estimated the parameter of the market price of risk  $\theta(x)$ , and have analysed empirically the noise residual  $dW_t(x)$  expressed as  $\epsilon_t(x) = \sigma(x)\tilde{\epsilon}_t(x)$  in a discrete form in (7). The purpose of this Section is to recover an infinite dimensional model for  $W_t(x)$  based on our findings.

To this end, we recall that  $\mathcal{H}$  is a separable Hilbert space of real-valued functions on  $\mathbb{R}_+$ , where  $W_t$  is a martingale process. As suggested by the notation, a first model could simply be to assume that  $W$  is a  $\mathcal{H}$ -valued Wiener process. However, this would mean that we expect  $t \mapsto W_t(x)$  to be a Gaussian process for each  $x \geq 0$ , which is at stake with our empirical findings showing clear non-Gaussian (or, coloured noise) residuals. After explaining the Samuelson effect, the residuals could be modelled nicely by a NIG distribution.

In stochastic modelling of financial price dynamics, it is common to scale the random variations by a volatility factor. We follow this idea, and propose a model of  $W$  of the form

$$W_t = \int_0^t \Sigma_s dL_s, \quad (11)$$

where  $s \mapsto \Sigma_s$  is an  $L(\mathcal{U}, \mathcal{H})$ -valued predictable process and  $L$  is a  $\mathcal{U}$ -valued Lévy process with zero mean and finite variance. We refer to (Peszat and Zabczyk, 2007, Sect. 8.6) for conditions to make the stochastic integral well-defined. As a first case, we can choose  $\Sigma_s \equiv \Psi$  time-independent, being an operator mapping elements of the separable Hilbert space  $\mathcal{U}$  into  $\mathcal{H}$ . An increment in  $W_t$  can be approximated (based on the definition of the

447 stochastic integral, see (Peszat and Zabczyk, 2007, Ch. 8)) as

$$W_{t+\Delta t} - W_t \approx \Psi(L_{t+\Delta t} - L_t) \quad (12)$$

448 Choose now  $\mathcal{U} = L^2(\mathbb{R})$ , the space of square integrable functions on the real line equipped  
 449 with the Lebesgue measure, and assume  $\Psi$  is an integral operator on  $L^2(\mathbb{R})$ , i.e., for  
 450  $g \in L^2(\mathbb{R})$ , the mapping

$$\mathbb{R}_+ \ni x \mapsto \Psi(g)(x) = \int_{\mathbb{R}} \tilde{\sigma}(x, y)g(y) dy \quad (13)$$

451 defines an element in  $\mathcal{H}$ . Furthermore, if  $\text{supp } \tilde{\sigma}(x, \cdot)$  is concentrated in a close neighbor-  
 452 hood of  $x$ , we can further make the approximation  $\Psi(g)(x) \approx \tilde{\sigma}(x, x)g(x)$ . As a result,  
 453 we find

$$W_{t+\Delta t}(x) - W_t(x) \approx \tilde{\sigma}(x, x)(L_{t+\Delta t}(x) - L_t(x)). \quad (14)$$

454 In view of the definition of  $\epsilon_t(x)$  in (7), we can choose  $\sigma(x) = \tilde{\sigma}(x, x)$  to be the model for  
 455 the Samuelson effect that we identified and discussed in Subsect. 4.2, and we let  $L_t$  be a  
 456 NIG Lévy process with values in  $L^2(\mathbb{R})$  to model the standardized residuals  $\tilde{\epsilon}_t$  (see Benth  
 457 and Krühner (2015) for a definition of such a process).

Recall from Fig. 10 the spatial correlation structure of  $\tilde{\epsilon}_t(x)$ . This provides the empirical foundation for defining a covariance functional  $\mathcal{Q}$  associated with the Lévy process  $L$ . In general, we know that for any  $g, h \in L^2(\mathbb{R})$ ,

$$\mathbb{E}[(L_t, g)_2(L_t, h)_2] = (\mathcal{Q}g, h)_2$$

458 where  $(\cdot, \cdot)_2$  denotes the inner product in  $L^2(\mathbb{R})$  (see (Peszat and Zabczyk, 2007, Thm. 4.44)).

459 The covariance functional will be a symmetric, positive definite trace class operator from



460  $L^2(\mathbb{R})$  into itself. It can be specified as an integral operator on  $L^2(\mathbb{R})$  by

$$461 \quad \mathcal{Q}g(x) = \int_{\mathbb{R}} q(x, y)g(y) dy, \quad (15)$$

462 for some suitable “kernel-function”  $q$ . If  $q$  is symmetric, positive definite and continuous  
 463 function, then it follows from Thm. A.8 in Peszat and Zabczyk (2007) that  $\mathcal{Q}$  is a covari-  
 464 ance operator of  $L$  if we restrict ourselves to  $L^2(\mathcal{O})$ , where  $\mathcal{O}$  is a bounded and closed  
 465 subset of  $\mathbb{R}$ . Indeed, we can think of  $\mathcal{O}$  as the maximal horizon of the market, in terms  
 466 of relevant times to maturity (recall that we have truncated the forward curves in our  
 empirical study to a horizon of 2 years).

467 If we assume  $g \in L^2(\mathbb{R})$  to be close to  $\delta_x$ , the Dirac  $\delta$ -function, and likewise,  $h \in$   
 468  $L^2(\mathbb{R})$  being close to  $\delta_y$ ,  $(x, y) \in \mathbb{R}^2$ , we find approximately

$$\mathbb{E}[L_t(x)L_t(y)] = q(x, y). \quad (16)$$

469 This shows that we may interpret the function  $q$  as the spatial correlation function of  
 470  $L$ . Unfortunately, the Dirac  $\delta$ -function  $\delta_x$  is not an element in  $L^2(\mathbb{R})$ , so we can only  
 471 obtain the relationship in Equation (16) in an approximative manner. Note that we can  
 472 approximate  $\delta_x$  arbitrary well by smooth functions in  $L^2(\mathbb{R})$ , so for practical applications  
 473 we may use the relation in Equation (16). From the spatial correlation study of  $\tilde{\epsilon}_t$ , we  
 474 observe that the correlation is stationary in space in the sense that it only depends on the  
 475 distance  $|x - y|$ . Hence, with a slight abuse of notation, we let  $q(x, y) = q(|x - y|)$ . A simple  
 476 choice resembling to some degree the fast decaying property in Fig. 10 is  $q(|x - y|) =$   
 477  $\exp(-\gamma|x - y|)$  for a constant  $\gamma > 0$ . We further note that from Benth and Krühner (2015),  
 478 it follows that  $t \mapsto (L_t, g)_2$  is a NIG Lévy process on the real line. If  $g \approx \delta_x$ , then we see  
 479 that  $L_t(x)$  for given  $x$  is a real-valued NIG Lévy process. With these considerations, we  
 480 have established a possible model for  $W$  which is, at least approximately, consistent with  
 481 our empirical findings for  $\epsilon_t$ .

Let us briefly discuss why we suggest to use  $\mathcal{U} = L^2(\mathbb{R})$  and introduce a rather complex integral operator definition of  $\Psi$ . As mentioned in Sect. 2, the Hilbert space  $\mathcal{H}$  to realize the deseasonalized forward price dynamics  $f_t$  should be a function space on  $\mathbb{R}_+$ .  $L^2(\mathbb{R})$  is a space of equivalence classes, and the evaluation operator  $\delta_x(g) = g(x)$  is not a continuous linear operator on this space. A natural Hilbert space where indeed  $\delta_x$  is a linear functional (e.g., continuous linear operator from the Hilbert space to  $\mathbb{R}$ ) is the so-called Filipovic space. The Filipovic space was introduced and studied in the context of interest rate markets by Filipovic (2001), while Benth and Krühner (2014, 2015) have proposed this as a suitable space for energy forward curves. From Benth and Krühner (2014) we have a characterization of the possible covariance operators of Lévy processes in the Filipovic space, which, for example, cannot be stationary in the form suggested for  $q$  above. Using  $\mathcal{U} = L^2(\mathbb{R})$  opens for a much more flexible specification of the covariance operator, which matches nicely the empirical findings on our electricity data. On the other hand, we need to bring the noise  $L$  over to the Filipovic space, since we wish to have dynamics of the term structure in a Hilbert space for which we can evaluate the curve at a point  $x \geq 0$ , that is,  $\delta_x(f_t) = f_t(x)$  makes sense. We recover the actual forward price dynamics  $t \mapsto F(t, T)$  in this case by

$$F(t, T) = f(t, T - t) = \delta_{T-t}(f_t).$$

482 We remark that for elements  $f$  in the Filipovic space,  $x \mapsto f(x)$  will be continuous, and  
483 weakly differentiable. To specify  $\Psi$  as an integral operator on  $L^2(\mathbb{R})$ , we can bring any  
484 element of  $L^2(\mathbb{R})$  to a smooth function. Indeed, the convolution product of a square  
485 integrable function with a smooth function will yield a smooth function (see (Folland,  
486 1984, Prop. 8.10)). This enables us to select "volatility" functions  $\tilde{\sigma}$  ensuring that  $W_t$   
487 becomes an element of the Filipovic space. Unfortunately, a simple multiplication operator  
488  $\Psi(g)(x) = \sigma(x)g(x)$  will not do the job, as this will not be an element of the Filipovic  
489 space for general  $g \in L^2(\mathbb{R})$ . In conclusion, with  $\mathcal{H}$  being the Filipovic space, we choose a

490 different space for the noise  $L$  to open up for flexibility in modelling the spatial correlation,  
 491 and an integral operator for  $\Psi$  to ensure that we map the noise into the Filipovic space,  
 492 at the same time modeling the Samuelson effect.

493 To follow up on the integral operator, we know the function  $\tilde{\sigma}(x, y)$  on the diagonal  
 494  $x = y$ , since here we want to match with the observed curve for the Samuelson effect. In  
 495 a neighborhood around  $x$ , we smoothly interpolate to zero such that  $\tilde{\sigma}(x, \cdot)$  has a support  
 496 close to  $\{x\}$ , and such that the function defines an integral operator being sufficiently  
 497 regular. One possibility is to define  $\tilde{\sigma}(x, y) = \eta(x)\bar{\sigma}(|x - y|)$ , where  $\bar{\sigma} : \mathbb{R}_+ \rightarrow \mathbb{R}_+$  is  
 498 smooth,  $\bar{\sigma}(0) = 1$ , and  $\text{supp } \bar{\sigma}$  is the interval  $(-a, a)$  for  $a$  small. With this definition, we  
 499 have that  $\eta$  models the Samuelson effect, the operator  $\Psi$  is a convolution product with  $\bar{\sigma}$ ,  
 500 followed by a multiplication with  $\eta$ . With  $\eta$  being an element of the Filipovic space, we  
 501 have specified  $\Psi$  as desired. By inspection of the curve for the volatility term structure  
 502 in Figure 4, a first-order approximation of it could be a function  $\eta(x) = a \exp(-\zeta x) + b$ ,  
 503 for constants  $a, \zeta$  and  $b$ , where  $b > 0$  is the long-term level and  $\zeta > 0$  measures the  
 504 exponential decay in the short end. We note that  $\eta(0) = a + b$  will be the spot volatility.  
 505 With such a specification,  $\eta$  will be an element of the Filipovic space since it is smooth and  
 506 asymptotically constant. As we see, this simple model fails to account for the pronounced  
 507 bumps in the curve that we have discussed earlier. By a more sophisticated model, one  
 508 can take these into account as well.

509 Our empirical analysis also show indications of stochastic volatility effects. We will  
 510 not discuss possible GARCH/ARCH specifications in continuous time, but briefly just  
 511 mention that we can choose  $\Sigma_s = V_s \Psi$ , where  $s \mapsto V_s$  is a  $\mathbb{R}_+$ -valued stochastic process.  
 512 For example, we can define  $V$  to be the Heston stochastic volatility dynamics (see Hes-  
 513 ton (1993)) or the BNS stochastic volatility model (see Barndorff-Nielsen and Shephard  
 514 (2001)). In this case, it would be natural to suppose  $L$  to be a Wiener process in  $L^2(\mathbb{R})$ ,  
 515 since the additional stochastic volatility process  $V$  will induce non-Gaussian distributed  
 516 residuals. We leave the further discussion on stochastic volatility models in infinite di-

517 mensional term structure models for future research (see however, Benth, Rüdiger, and  
518 Süss (2015) for a Hilbert-valued Ornstein-Uhlenbeck processes with stochastic volatility).

## 519 **7 Conclusion and future work**

520 In this study, we derived a spatio-temporal dynamical model based on the Heath-Jarrow-  
521 Morton (HJM) approach under the Musiela parametrization (see Heath, Jarrow, and  
522 Morton (1992)), which ensures an arbitrage-free model for electricity forward prices. A  
523 discretized version of the model has been fitted to electricity forward prices to examine  
524 the probabilistic characteristics of the data. We disentangled the seasonal pattern from  
525 the market price of risk and random perturbations of prices and analysed empirically their  
526 statistical properties.

527 As a special feature of our model, we further disentangled the temporal from spatial  
528 (time to maturity) effects on the dynamics of forward prices, which marks one of the main  
529 contributions of this study to the academic literature (see Andresen, Koekebakker, and  
530 Westgaard (2010)). After filtering out both temporal and spatial effects of price forward  
531 curves and the market price of risk, we estimated the term structure volatility. Finally, our  
532 model residuals show a white-noise pattern, which validates our modeling assumptions.

533 The model has been fitted to a unique data set of historical daily PFCs for the  
534 German electricity market. We firstly performed a deseasonalization of the initial curves,  
535 where the seasonal component takes into account typical deterministic dynamics observed  
536 in the German electricity prices (see Paraschiv, Fleten, and Schürle (2015), Paraschiv  
537 (2013)). We further estimated the risk premia in the deseasonalized curves (stochastic  
538 component) and examined, in this context, the distribution of the noise: term structure  
539 volatility and its spatio-temporal correlations structures. Our results show that the short-  
540 term risk premia oscillate around zero, but become negative in the long run, which is  
541 consistent with the empirical literature (Paraschiv, Fleten, and Schürle (2015), Burger,

542 Graeber, and Schindlmayr (2007)). We found that the noise marginals are coloured-noise  
543 with a strong leptokurtic pattern and heavy-tails, which have been successfully modeled  
544 by a normal inverse Gaussian distribution (NIG). There were signs of stochastic volatility  
545 effects as well. The high performance of the NIG distribution in modeling the noise  
546 marginals of forward electricity prices confirms previous findings of Frestad, Benth, and  
547 Koekebakker (2010). The term structure of volatility decays overall with increasing time  
548 to maturity, a typical Samuelson effect. However, the term structure of volatility in our  
549 data set has additionally clear bumps around the maturity of 1 month and third quarter,  
550 both being related to an increased activity in the market for the corresponding futures  
551 contracts. Our analysis also detects a fast decaying pattern in the spatial correlations as  
552 a function of distance between times to maturity.

553 Our empirical findings mark an additional contribution over existing related lit-  
554 erature Andresen, Koekebakker, and Westgaard (2010): we shed light on the statistical  
555 properties of risk premia, of the noise, volatility term structure and of the spatio-temporal  
556 noise correlation structures. Notably, we look at price residuals where the maturity effect  
557 is corrected for, unlike the approach of Andresen, Koekebakker, and Westgaard (2010).

558 Based on the empirical insights, we revisited the spatio-temporal model of forward  
559 prices and derived a mathematical model for the noise. After explaining the Samuelson  
560 effect in the volatility term structure, the residuals are modeled by an infinite dimensional  
561 NIG Lévy process, which allows for a natural formulation of a covariance functional. We  
562 model, in this way, the typical fat tails and fast-decaying pattern of spatial correlations.  
563 Still, our empirical findings show some slight remaining volatility clustering effects in  
564 the standardized residuals, which can be described by a stochastic volatility model for-  
565 mulation. However, we will discuss and develop stochastic volatility models in infinite  
566 dimensional term structure models in future research.

## Acknowledgements

Fred Espen Benth acknowledges financial support from the project FINEWSTOCH, funded by the Norwegian Research Council. The authors thank very much Gido Haarbrücker, Claus Liebenberger and Michael Schürle from the Institute for Operations Research and Computational Finance, University of St. Gallen, for the continued support in the data collection step of this work. We are grateful to the reviewers for constructive feedback on our paper, resulting in a significant improvement in the presentation of our analysis.

## References

- ANDRESEN, A., S. KOEKEBAKKER, AND S. WESTGAARD (2010): “Modeling electricity forward prices using the multivariate normal inverse Gaussian distribution,” *The Journal of Energy Markets*, 3(3), 3–25.
- AUDET, A., P. HEISKANEN, J. KEPPO, AND A. VEHVILÄINEN (2004): “Modeling electricity forward curve dynamics in the Nordic market,” in *Modelling Prices in Competitive Electricity Markets*, ed. by D. W. Bunn, pp. 251–265. Wiley, Chichester.
- BARNDORFF-NIELSEN, O. E., F. E. BENTH, AND A. VERAART (2013): “Modelling energy spot prices by volatility modulated Lévy-driven Volterra processes,” *Bernoulli*, 19, 803–845.
- (2014): “Modelling electricity futures by ambit fields,” *Advances in Applied Probability*, 46, 719–745.
- (2015): “Cross-commodity modelling by multivariate ambit fields,” in *Commodities, Energy and Environmental Finance, Fields Institute Communications Series*, ed. by R. Aid, M. Ludkovski, and R. Sircar, pp. 109–148. Springer Verlag.
- BARNDORFF-NIELSEN, O. E., AND N. SHEPHARD (2001): “Non-Gaussian Ornstein-Uhlenbeck-based models and some of their uses in economics,” *Journal of the Royal Statistical Society, Series B*, 63, 167–241.
- BARTH, A., AND F. E. BENTH (2014): “The forward dynamics in energy markets – infinite dimensional modeling and simulation,” *Stochastics*, 86, 932–966.
- BENTH, F.-E., J. KALLSEN, AND T. MEYER-BRANDIS (2007): “A non-Gaussian Ornstein-Uhlenbeck process for electricity spot price modeling and derivatives pricing,” *Applied Mathematical Finance*, 14, 153–169.

- 597 BENTH, F. E., C. KLÜPPELBERG, G. MÜLLER, AND L. VOS (2014): “Futures pricing  
598 in electricity markets based on stable CARMA spot models,” *Energy Economics*, 44,  
599 392–406.
- 600 BENTH, F. E., AND S. KOEKEBAKKER (2008): “Stochastic modeling of financial elec-  
601 tricity contracts,” *Energy Economics*, 30, 1116–1157.
- 602 BENTH, F. E., S. KOEKEBAKKER, AND F. OLLMAR (2007): “Extracting and applying  
603 smooth forward curves from average-based commodity contracts with seasonal varia-  
604 tion,” *Journal of Derivatives*, 15, 52–66.
- 605 BENTH, F. E., AND P. KRÜHNER (2014): “Representation of infinite-dimensional for-  
606 ward price models in commodity markets,” *Communications in Mathematics and Statis-  
607 tics*, 2, 47–106.
- 608 ——— (2015): “Derivatives pricing in energy markets: an infinite dimensional ap-  
609 proach,” *SIAM Journal on Financial Mathematics*, 6, 825–869.
- 610 BENTH, F. E., AND P. KRÜHNER (2015): “Subordination of Hilbert space valued Lévy  
611 processes,” *Stochastics*, 87, 458–476.
- 612 BENTH, F. E., AND J. LEMPA (2014): “Optimal portfolios in commodity markets,”  
613 *Finance & Stochastics*, 18, 407–430.
- 614 BENTH, F. E., B. RÜDIGER, AND A. SÜSS (2015): “Ornstein-Uhlenbeck processes in  
615 Hilbert space with non-Gaussian stochastic volatility,” *Submitted manuscript. Available  
616 on arXiv:1506.07245*.
- 617 BENTH, F. E., J. ŠALTYTĖ BENTH, AND S. KOEKEBAKKER (2008): *Stochastic Mod-  
618 elling of Electricity and Related Markets*. World Scientific, Singapore.
- 619 BLOECHLINGER, L. (2008): *Power prices – a regime-switching spot/forward price model  
620 with Kim filter estimation*, Dissertation of the University of St. Gallen, No. 3442.
- 621 BURGER, M., B. GRAEBER, AND G. SCHINDLMAYR (2007): *Managing Energy Risk –  
622 An Integrated View on Power and Other Energy Markets*. Wiley.
- 623 CALDANA, R., G. FUSAI, AND A. RONCORONI (2016): “Energy forward curves with  
624 thin granularity,” Available at SSRN: abstract=2777990.
- 625 CARTEA, A., AND M. FIGUEROA (2005): “Pricing in electricity markets: a mean revert-  
626 ing jump diffusion model with seasonality,” *Applied Mathematical Finance*, 12, 313–335.

- 627 CLEWLOW, L., AND C. STRICKLAND (2000): *Energy Derivatives: Pricing and Risk*  
628 *Management*. Lacima Publications, London.
- 629 FILIPOVIC, D. (2001): *Consistency Problems for Heath-Jarrow-Morton Interest Rate*  
630 *Models*. Springer Verlag, Berlin Heidelberg.
- 631 FLETEN, S.-E., AND J. LEMMING (2003): “Constructing forward price curves in elec-  
632 tricity markets,” *Energy Economics*, 25, 409–424.
- 633 FOLLAND, G. (1984): *Real Analysis*. John Wiley & Sons, New York.
- 634 FRESTAD, D. (2008): “Common and unique factors influencing daily swap returns in the  
635 Nordic electricity market, 1997–2005,” *Energy Economics*, 30, 1081–1097.
- 636 FRESTAD, D., F. BENTH, AND S. KOEKEBAKKER (2010): “Modeling term structure  
637 dynamics in the Nordic electricity swap market,” *Energy Journal*, 31, 53–86.
- 638 GARCIA, I., C. KLÜPPELBERG, AND G. MÜLLER (2011): “Estimation of Stable CARMA  
639 Models with an Application to Electricity Spot Prices,” *Statistical Modelling*, 11, 447–  
640 470.
- 641 GEMAN, H. (2005): *Commodities and Commodity Derivatives: Modeling and Pricing for*  
642 *Agriculturals, Metals and Energy*, The Wiley Finance Series. John Wiley and Sons.
- 643 GOLDSTEIN, R. S. (2000): “The Term Structure of Interest Rates as a Random Field,”  
644 *Review of Financial Studies*, 13, 365–384.
- 645 HEATH, D., R. JARROW, AND A. MORTON (1992): “Bond pricing and the term structure  
646 of interest rates: a new methodology for contingent claim valuation,” *Econometrica*,  
647 60, 77–105.
- 648 HESTON, S. (1993): “A closed-form solution for options with stochastic volatility with  
649 applications to bond and currency options,” *Review of Financial Studies*, 6, 327–343.
- 650 KENNEDY, D. P. (1994): “The term structure of interest rates as a Gaussian random  
651 field,” *Mathematical Finance*, 4, 247–258.
- 652 KIESEL, R., G. SCHINDLMAYR, AND R. BOERGER (2009): “A two-factor model for the  
653 electricity forward market,” *Quantitative Finance*, 9, 279–287.
- 654 KOEKEBAKKER, S., AND F. OLLMAR (2005): “Forward curve dynamics in the Nordic  
655 electricity market,” *Managerial Finance*, 31, 73–94.



- 656 LUCIA, J. J., AND E. S. SCHWARTZ (2002): “Electricity prices and power derivatives:  
657 evidence from the Nordic power exchange,” *Review of Derivatives Research*, 5, 5–50.
- 658 PARASCHIV, F. (2013): “Price dynamics in electricity markets,” in *Risk Management in*  
659 *Energy Production and Trading*, ed. by P. G. Kovacevic, R.M., and M. Vespucci, pp.  
660 57–111. Springer.
- 661 PARASCHIV, F., D. ERNI, AND R. PIETSCH (2014): “The impact of renewable energies  
662 on EEX day-ahead electricity prices,” *Energy Policy*, 73, 196–210.
- 663 PARASCHIV, F., S.-E. FLETEN, AND M. SCHÜRLE (2015): “A spot-forward model for  
664 electricity prices with regime shifts,” *Energy Economics*, 47, 142–153.
- 665 PERRON, P., AND S. NG (1996): “Useful modifications to some unit root tests with  
666 dependent errors and their local asymptotic properties,” *Review of Economic Studies*,  
667 63, 435–463.
- 668 PESZAT, S., AND J. ZABCZYK (2007): *Stochastic Partial Differential Equations with Lévy*  
669 *Noise*. Cambridge University Press, Cambridge.
- 670 PIETZ, M. (2009): “Risk premia in electricity wholesale spot markets empirical evidence  
671 from Germany,” *Working Paper, Center for Entrepreneurial and Financial Studies.*  
672 *Technical University of Munich*.
- 673 RONCORONI, A., AND H. GEMAN (2006): “Understanding the fine structure of electricity  
674 prices,” *Journal of Business*, 79, 1225–1261.
- 675 RONCORONI, A., AND P. GUIOTTO (2001): “Theory and Calibration of HJM with Shape  
676 Factors,” *Mathematical Finance, Springer Finance*, pp. 407-426.
- 677 WERON, R., AND S. BORAK (2008): “A semiparametric factor model for electricity  
678 forward curve dynamics,” *Journal of Energy Markets*, 1, 3–16.
- 679 WERON, R., AND M. ZATOR (2014): “Revisiting the relationship between spot and  
680 futures prices in the Nord Pool electricity market,” *Energy Economics*, 44, 178–190.
- 681 WRIGHT, J. H. (1999): “Testing for a unit root in the volatility of asset returns,” *Journal*  
682 *of applied econometrics*, 14, 309–318.